Bullet Impact on Armox600T Armored Plate - Simulation and Experiments

Attapon C* and Ekaratch P

Defence Technology Institute, 47/433 Moo3 Banmai, Pakkret, Nonthaburi, 11120
*Corresponding Author: attapon.c@dti.or.th, 0-2980-6198, 0-2980-6688 ext300

Abstract

In order to study and investigate the shielding efficiency of the armored vehicle design, the computational and experimental simulations of M193 bullet impact on Armox600T armored plate were conducted. M193 bullet is rifle cartridge with medium level of armor piecing treat, whereas Armox600T is globally applied in military armored vehicle. Therefore, they are the promising selection for the initial study and investigation of the bullet impact on the armored plate.

For the computational simulation, the two dimensional explicit nonlinear code was selected to predict the crater geometry, depth, and diameter owning to bullet impacting on the Armox600T plate, while in the case of the experimental investigation, shooting five bullets on the armored plate according to the military ballistic test standard was performed. The computational and experimental results showed that no complete penetrations were observed. The prediction of the geometry and size of forming crater in terms of depth and diameter based on the experiment and computation were agreed well.

Keywords*:* Rifle, Armor Piecing, Explicit nonlinear, Crater, Penetration simulation

1. Introduction

In combat vehicle, armored plate is essential to protect the soldiers. Therefore, accuracy of bullet penetrating prediction for armor vehicle design is highly important. However, there are only few analytical models describing the bullet penetration such as the Walker-Anderson[1] and Schmidt-Holsapple equations[2]. For Walker-Anderson penetration model, the centerline momentum balance is applied to predict the penetration of long rods into semi-finite metallic target. The numerical approach is needed to compute crater, bulging, and perforation shape. The Schmidt-Holsapple equation is formulated from the experiments and given below

$$d = 2.06t\left(\frac{\rho_P}{\rho_t}\right)^{-0.159}\left(\frac{2.68F_{tu}}{\rho_P V_n^2}\right)^{0.236} \quad (1)$$

Where d = Bullet diameter (in)

t = Armored plate thickness (in)

ρ_P, ρ_t = Bullet and armored plate density (lb/in^3) respectively

F_{tu} = Ultimate tensile strength of armored plate (lb/in^2)

V_n = Impact velocity of bullet (ft/s)

When the armored plate material has ultimate tensile strength equal to 2000MPa, bullet diameter 7.8 mm, material density of both armored plate and bullet are 7.8 mm, we could plotted the relation between armored plate thickness and impact velocity as shown in the figure 1.

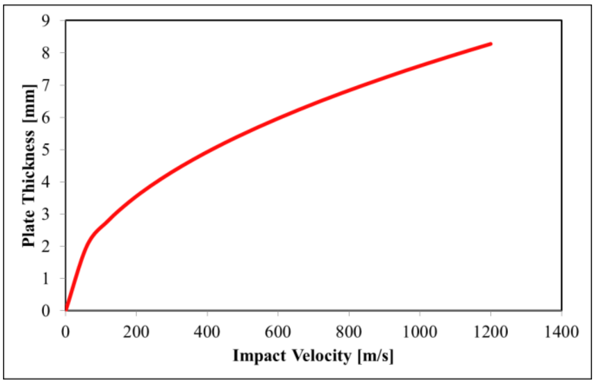

Fig. 1 Relation between plate thickness and bullet impact velocity

This relation gives us the preliminary determinate the minimum plate thickness for using against the known bullet type.

Since the previous investigation of bullet penetration is relied on the analytical model, this paper thus presents the computation and experimentation to investigate the physics of bullet penetration in detail.

2. Computer Modeling

The M193 bullet rifle cartridge with medium level of armor piecing treat is used in this investigation and consisted mainly of two portions, lead and copper case as depicted in Fig. 1. In order to reduce the computational task, the two-dimensional axisymmetric model is introduced. The quadrilateral cells are constructed throughout the bullet (Fig. 2). The total numbers of cells are 27,600 elements.

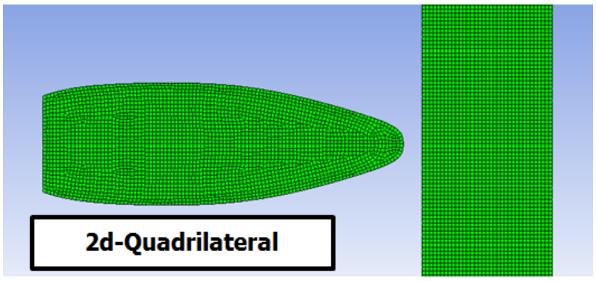

Fig. 2 Computational modeling and 2d meshing

The maximum velocity (970 m/s) of bullet is imposed as the boundary condition. Since Armox600T is the armored protection plate globally applied to military vehicle, we then selected the Armox600T plate for the target of bullet impact. We expected that this is the promising selection for the initial study and investigation of the bullet impact on the armored plate. The Schmidt-Holsapple equation was conducted to predict the thickness of the Armox600T plate, which is 7 mm. For computational simulation, the two dimensional explicit nonlinear code of Autodyne was applied. The explicit nonlinear materials of copper, lead, and Armox600T are used to model the elastic and plastic deformations.

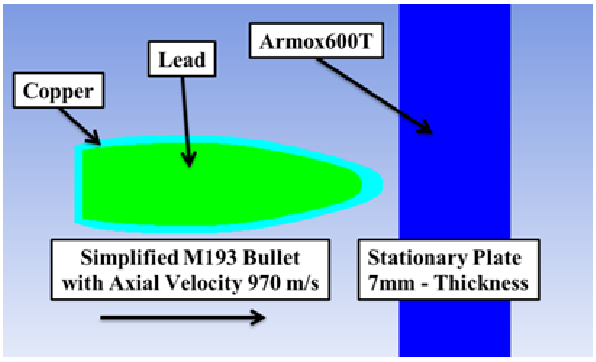

Fig. 3 Computational Boundary Condition

3. Material Modeling

Material model for numerical modeling, The Jonhson & Cook strength model had been used to express the relation of strength on strain. The equation is given by

$$\sigma_Y = \left[A + B\varepsilon^n\right]\left[1 + C\ln\frac{\dot{\varepsilon}}{\dot{\varepsilon}_0}\right]\left[1 - \left(\frac{T - T_0}{T_{melt} - T_0}\right)^m\right] \quad (2)$$

Where A, B, C, m and n are constant parameter which found from experiment, $\dot{\varepsilon}$ and $\dot{\varepsilon}_0$ are strain rate, T_0 and T_{melt} are reference temperature and melting temperature respectively. The material model for Armox600T [3] used in this simulation was shown in Table.1 and the other material , copper and lead, were shown in Table.2 and Table.3 respectively.

Table. 1 Material Model for ARMOX600T

Parameter	Value	Unit
Density	7800	kg/m^3
Specific Heat	477	J/kg/C
Johnson Cook Strenght		
Strain rate correction	first-order	
Initial Yield Stress	1500	MPa
Hardening Constant	515.2	MPa
Hardening Exponent	0.057	
Strain Rate Constant	0.014	
Thermal Softening Exponent	1	
Melting Temperature	1800	K
Reference Strain Rate	1	
Shear Modulus	81800	MPa
Shock EOS Linear		
Gruneisen Coefficient	2.17	
Parameter C1	4569	m/s
Parameter S1	1.49	
Parameter Quadratic S2	0	s/m

Table. 2 Material Model for Copper

Parameter	Value	Unit
Density	8900	kg/m^3
Specific Heat	1.00E-12	J/kg/C
Multilinear Isotropic Hardening		
Shear Modulus	46400	MPa
Shock EOS Linear		
Gruneisen Coefficient	2	
Parameter C1	3958	m/s
Parameter S1	1.497	
Parameter Quadratic S2	0	s/m

Table. 3 Material model for Lead

Parameter	Value	Unit
Density	11340	kg/m^3
Specific Heat	124	J/kg/C
Steinberg Guinan		
Initial Yield Stress	8	MPa
Hardening Constant	110	MPa
Maximum Yield Stress Ymax	100	MPa
Hardening Exponent	0.52	
Derivative dG/dP	1	
Derivative dG/dT	-9.976	Mpa/C
Melting Temperature	487	C
Shear Modulus	8600	MPa
Shock EOS Linear		
Gruneisen Coefficient	2.74	
Parameter C1	2006	m/s
Parameter S1	1.429	
Parameter Quadratic S2	0	s/m

4. Computational Result

A simulation showed that when the bullet impacted the plate the outer shell of bullet was peeled off and shattered into many pieces while the inside core try to penetrate into the plate. At the centerline, the maximum concentration stress occurred and the material of plate could not resist this stress which yielded a result of crater (at front of plate) and bulge (at rear of plate) formulation. The simulation time took about 300 μ s which the velocity of bullet was zero so that this point is the end of computation.

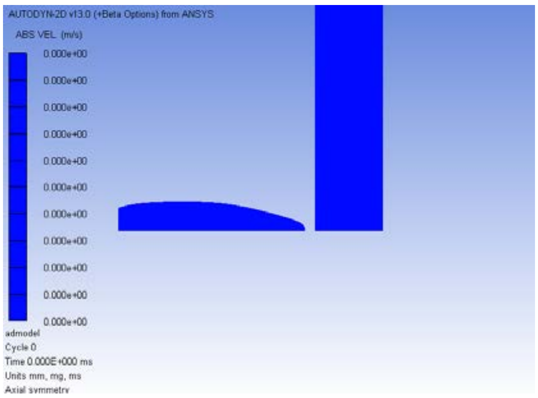

Fig. 4 Computation Time 0 μ s, Start of Computation(Color represent the absolute velocity in m/s)

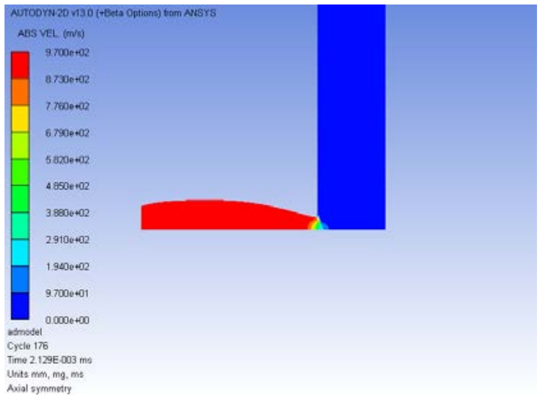

Fig. 5 Computation Time 21 μ s

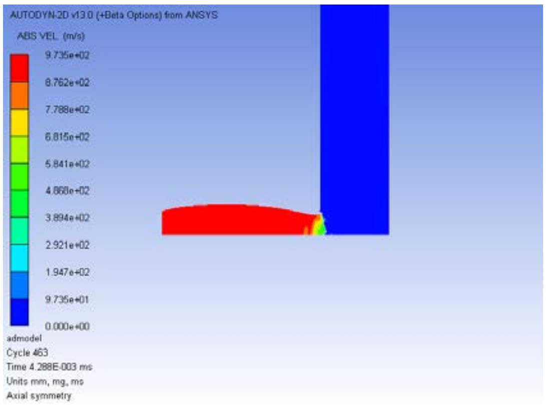

Fig. 6 Computation Time 42 μ s

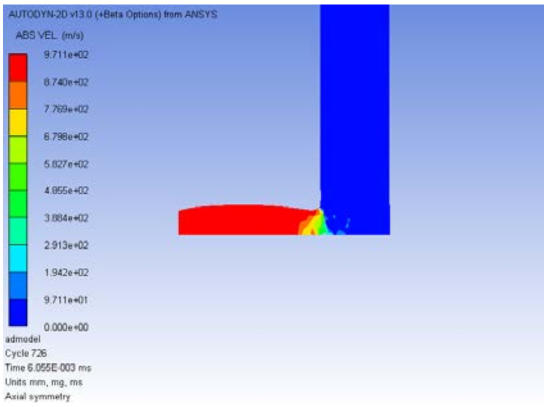

Fig. 7 Computation Time 60 μ s

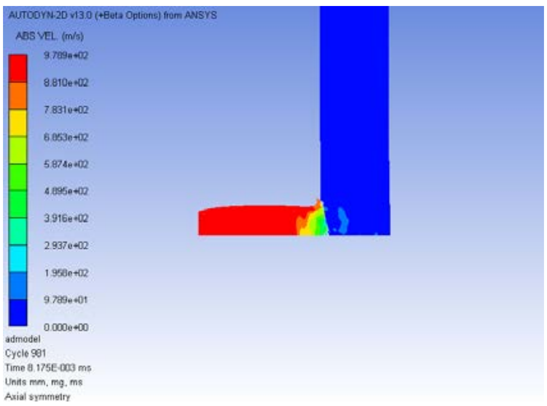

Fig. 8 Computation Time 81 μ s

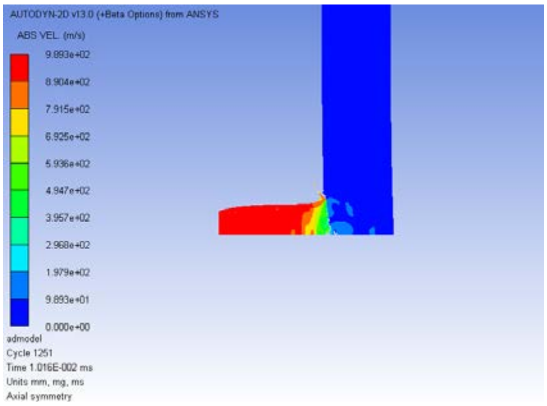

Fig. 9 Computation Time 101 μ s

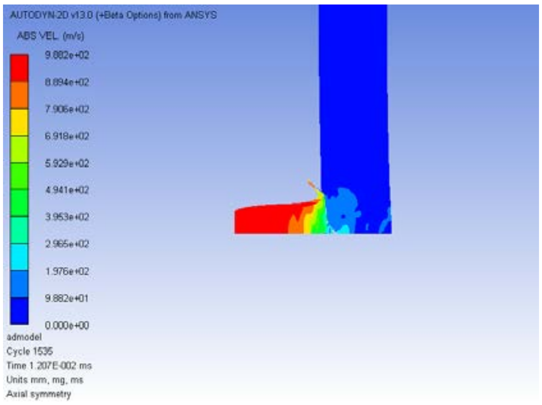

Fig. 10 Computation Time 120 μ s

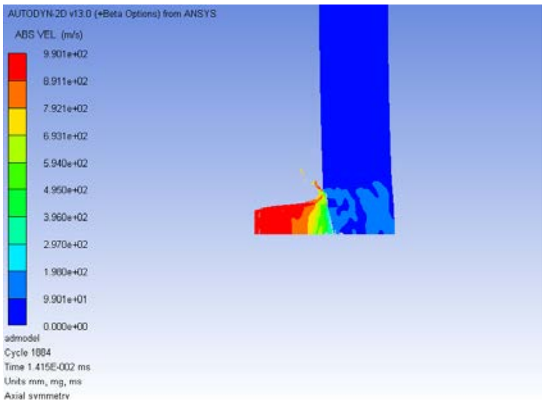

Fig. 11 Computation Time 141 μ s

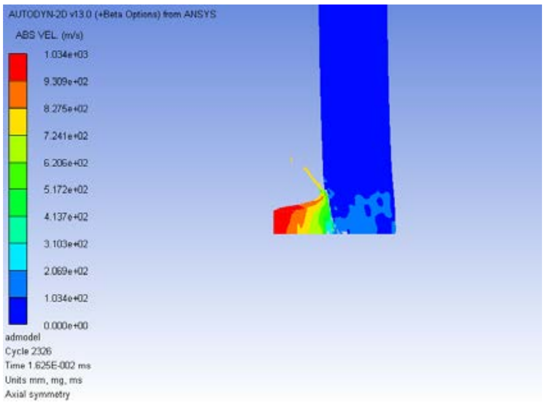

Fig. 12 Computation Time 162 μ s

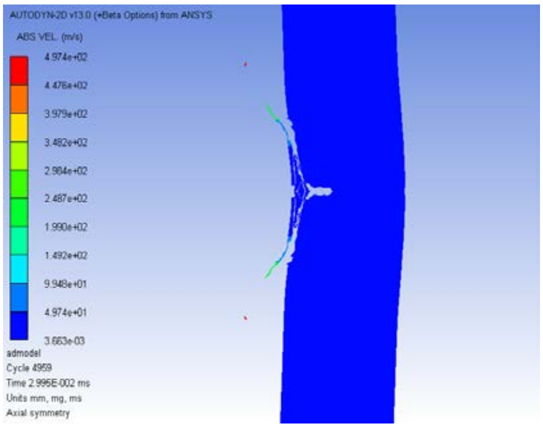

Fig. 13 Computation Time 300 μ s, End of Computation

5. Result Comparison and Discussion

Fig. 14 and 15 depicted the crater depth obtained from the computation and experiment. The computational and experimental results showed that no complete penetration is observed. The prediction of the geometry and size of forming crater in terms of depth and diameter based on the computation and experiment are agreed well. The experimental depth and diameter of crater are 1.52 mm and 9.65 mm, respectively, while the computational depth and diameter of crater are 1.21 mm and 9.15 mm respectively, which is in range of acceptable error for the primary study and investigation phase.

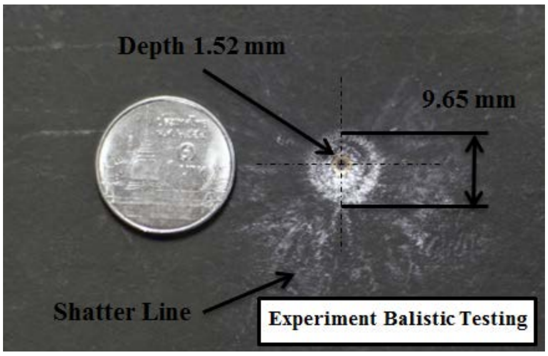

Fig. 14 Crater depth and Diameter from experiment

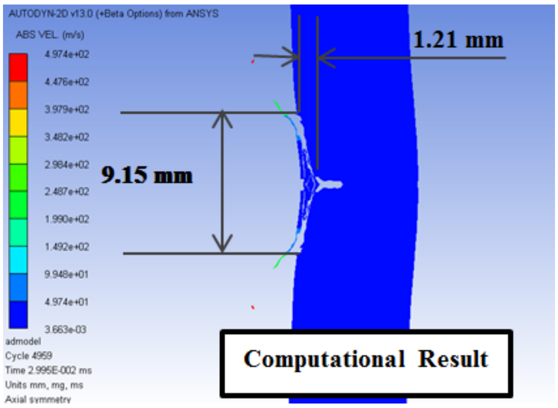

Fig. 15 Crater depth and Diameter from computational result

6. References

[1] S.Chocron, C.E. Anderson Jr, J.D. walker and M.Ravid (2003). A unified model for long-rod penetration in multiple metallic plates, *International Journal of Impact Engineering 28 (2003)*, pp. 391-411.

[2] K.B. Hayashida and J.H. Robinson (1991). Single Wall Penetration Equation, NASA TM-103565, *NASA technical memorundum* (1991).

[3] Martin Nilsson (2003). Constitutive Model for Armox500T and Armox600T at Low and Medium Strain Rates, FOI-R—1068—SE, Technical Report: Swedish Defence Research Agency.